IEEE Access
Multidisciplinary | Rapid Review | Open Access Journal

Received September 16, 2020, accepted October 6, 2020, date of publication October 12, 2020, date of current version October 22, 2020.

Digital Object Identifier 10.1109/ACCESS.2020.3030100

Model Predictive Control Approach for Optimal Power Dispatch and Duck Curve Handling Under High Photovoltaic Power Penetration

SULAIMAN S. AHMAD[1], (Student Member, IEEE), FAHAD SALEH AL-ISMAIL[1,3,4], (Senior Member, IEEE), ABDULLAH A. ALMEHIZIA[2], (Member, IEEE), AND MUHAMMAD KHALID[1], (Senior Member, IEEE)

[1]Electrical Engineering Department, Engineering College, King Fahd University of Petroleum and Minerals, Dhahran 31261, Saudi Arabia
[2]National Center for Electrical Systems Technology, Energy and Water Research Institute, King Abdulaziz City for Science and Technology, Riyadh 11442, Saudi Arabia
[3]Center for Environmental & Water, Research Institute, King Fahd University of Petroleum and Minerals, Dhahran 31261, Saudi Arabia
[4]K. A. CARE Energy Research & Innovation Center (ERIC), King Fahd University of Petroleum and Minerals, Dhahran 31261, Saudi Arabia

Corresponding author: Sulaiman S. Ahmad (g201705090@kfupm.edu.sa)

The authors would like to acknowledge the support provided by the Deanship of Scientific Research (DSR) at King Fahd University of Petroleum & Minerals (KFUPM) for funding this work through project No. DF181035. Also, the funding support provided by the K. A. CARE Energy Research & Innovation Center (ERIC).

ABSTRACT In this paper, an energy management system (EMS) has been developed based on model predictive control (MPC) to optimally dispatch the power units and particularly handle the duck curve fast ramping events. The methodology is specifically developed considering higher penetration of solar photovoltaic power subjected to realistic physical constraints. Battery energy storage, load shedding and solar curtailment have been utilized to effectively control the duck curve fast ramping events. The proposed system has been assessed with the help of a case study using a 24-bus RTS system. Consequently, detailed flexibility analyses were carried out and it has been proven that the given energy management and control system is capable of handling fast ramping events of duck curve. Furthermore, it has been observed that the overall operation cost of the system is also minimized. The performance of the developed model is compared with traditional non-MPC based mixed-integer linear programming approaches and it has been concluded that MPC-based optimization is more economical and effective in handling the duck curve challenges.

INDEX TERMS Battery energy storage system, curtailment, duck curve, model predictive control, photovoltaic, load shedding.

NOMENCLATURE

Parameters

η_{ch}	Charging efficiency of BESS.
η_{dis}	Discharging efficiency of BESS.
P_g^{max}	Maximum power generation of unit g.
P_g^{min}	Minimum power generation of unit g.
$P_{load,i}(k)$	Demand at bus i in time step k.
T	Total time.
Ut_g	Minimum up-time of unit g.
Dt_g	Maximum down-time of unit g.
R_g^{up}	Ramp-up of unit g.
R_g^{dn}	Ramp-down of unit g.
C_{shed}	Price penalty for load shedding.
C_{curt}	Price for solar PV curtailment.
$T_{PV,i}$	Solar PV Capacity at bus i.
$P_{PV,i}(k)$	Solar PV Power in time step k at bus i.
C_g^{up}	Start-up cost of generator g.
C_g^{dn}	Short-down cost of generator g.
$P_{net,i}(t)$	System net load in time instant t.
P_{ij}^{Rated}	Rated capacity of transmission lines.
E_i	BESS Capacity at bus i.
$P_{net}(t)$	Net load in time t.

Number Sets

N	Planning horizon.
N_g	Set of generators.
N_i	Set of buses.

The associate editor coordinating the review of this manuscript and approving it for publication was Qiuhua Huang.

Variables

TOC	Total operational cost.
$Fc_g(k)$	Fuel cost of unit g in time step k.
$Su_g(k)$	Start-up cost of unit g in time step k.
$Sd_g(k)$	Shut-down cost of unit g in time step k.
$P_g(k)$	Power generated by unit g in time step k.
$p_{pv,i}(k)$	PV power generated at bus i in time step k.
$P_{curt,i}(k)$	PV power curtailed in time step k.
$P_{shed,i}(k)$	Load shed at bus i in time step k.
$\delta_g(k)$	On/off status of unit g in time step k.
$y_g(k)$	Start-up status of unit g in time step k.
$z_g(k)$	Shut-down status of unit g in time step k.
$SoC_i(k)$	State of charge of the BESS at bus i in time k.
$P_{BESS,i}(t)$	BESS power at bus i in time step k.
$Pij(k)$	Power flow from bus i to bus j in time step k.
$P_{def}(t)$	Unblalanced net load in time t.
$Flex_{on}(t)$	System online flexibility in time t.
$Flex_{off}(t)$	System offline flexibility in time t.
$\theta_i(k)$	Voltage angle (rad) at bus i in time step k.
$R_{net}(t)$	System net load ramp in time t.
a_g, b_g, c_g	Fuel cost coefficients of unit g.

I. INTRODUCTION

Solar photovoltaic (PV) integration into power grids is on the rise [1], [2]. Solar PV has been widely adopted as it is relatively more available and more predictable than the other renewable energy sources (RESs). This has led to the high penetration of solar PV. The output of solar PV depends on the prevailing weather conditions. The solar PV can generate power only during the day and none after sunset because the output depends on solar irradiance. The output is usually at its peak during mid-day. With this behavior, high solar PV penetration causes the net load to exhibit a strange behaviour where the peak of the net electricity demand shifts from the day-time to the night. This cuts peak demand during the day-time which results in a very sharp increase in demand after sunset. This changes the shape of the net demand curve into the form of a duck shape known as the duck-curve. In this curve, there is a large gap between the day and night demands. This poses a great challenge in meeting the net demand. High penetration of RESs also leads to a new operating paradigm where the grid has too much RES without corresponding adequate demand. This leads to curtailment of the RES output which might be counterproductive [3]. The duck curve requires the use of more flexible and expensive power sources in order to smooth the sharp increase and decrease in the peaks. This raises another concern of flexibility of power system as the grid incorporates more PVs. In countries with high penetration of solar PV, unplanned stress on the electrical grid occurs regularly [4]. The National Renewable Energy Laboratory (NREL) made a report about the duck curve. The report pointed out the risk of over-generation posed by the duck curve with increased PV penetration [5]. It discusses in detail the level of PV curtailment needed to improve flexibility and pointed out the benefits of employing distributed resources to improve flexibility and reduce curtailment.

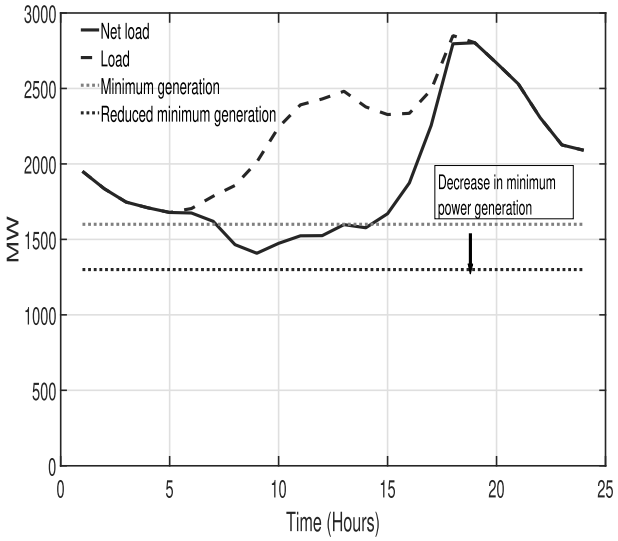

FIGURE 1. Duck curve fattening.

One of the main solutions for handling the duck curve ramps include PV curtailment. Curtailment involves decreasing the power output of wind or solar PV below the potential output. This may cause the overall benefits of adding more solar to fall to a point where additional installations are not worth the cost (Cochran *et al*. 2015) [6]. The duck curve only represents one day of the year and does not adequately show the amount of actual curtailment when there is an increase in the PV penetration, and does not show the effects of smoothing options. To this end, the authors of [7] proposed a technique of modelling probabilistic duck curve and probabilistic ramp curve using kernel density estimation, copula function, and dependent discrete convolution. According to the NREL report, the California ISO (CAISO) suggested two approaches to mitigating the effects of the duck-curve, namely, fattening and flattening the duck-curve. Fattening encompasses all the methods that lead to an increase in the flexibility of the power grid and gives room for continuous penetration of variable generation resources, for instance, the use of energy storage systems. It also involves decreasing the minimum power generation. This is illustrated in Figure 1. Flattening involves shrinking the ''belly'' shape of the duck curve. This basically involves demand response by shifting the supply/demand patterns, to allow solar to provide the energy demand that would not normally be present in the middle of the day as proposed by [5]. An example of duck curve flattening is shown in Figure 2. Other options that were proposed to address the duck-curve challenges include regional interchange of energy.

Energy storage system (ESS) is widely used for improving the flexibility of power systems. In power grids with high PV penetration, ESS have been used to provide flexibility. Managing ESS optimally is crucial to power system operation [8]. The authors of [9] proposed a model that uses electric

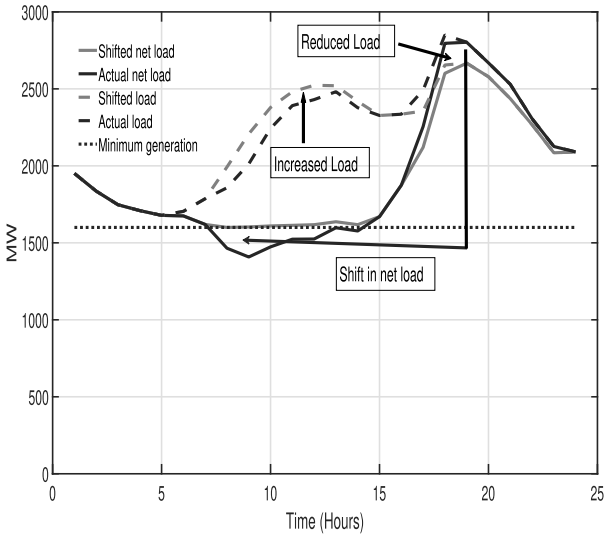

FIGURE 2. **Duck curve flattening.**

boilers for heat and pumped hydro storage to enable a higher penetration of renewable energy in China. The authors of [10] developed a microgrid scheme which uses PV. The potential energy from high rise buildings is used for mini hydro pump storage which shifts load from peak to off-peak periods. Chaudhary and Rizwan presented a technique that accommodates PV penetration through an energy management system (EMS) using pumped hydro storage and advanced PV forecast [11]. Floch *et al*. presented a distributed charging algorithm for plug-in electric vehicles to mitigate the duck curve challenges [12]. Recent works on handling duck-curve using ESS considered concentrated solar power (CSP) and pumped storage hydroelectricity (PSH) as ESS for handling the duck-curve peaks [13], [14]. PV curtailment is economically better solution to flexibility than ESS as shown by better results in dealing with flexibility issues, this is pointed out by Sevilla *et al*. [15]. Demand side management is also an option for handling flexibility requirements posed by high PV penetration. It involves shifting some of the loads from peak to off-peak times [16]. For instance, Sanandaji *et al*. propose a method of using thermostatically controlled loads such as air conditioners and refrigeration units to serve as fast regulation reserve service in the sunset thereby meeting some demand after sunset [17]. Lazar proposed an ''aggressive demand response'' as one of the strategies of dealing with duck curve challenges [18]. Demand-response programs are used to reduce load on the days when the stress on the system are not critical. Demand-response includes shedding some load when the power production is low. This is done at a cost which increases the total cost of operation.

This paper proposes a model for tackling the challenges posed by the duck-curve as a result of high PV penetration. This involves smoothing the duck curve using high flexibility product with an efficient EMS. The model minimizes the total operation cost of the power grid. Because the solar PVs depend on solar irradiance and ambient temperature [19], [20], their output is the highest during the day and zero after sunset. This might lead to under production by the grid after sunset and overproduction during peak periods of the PV output. One approach to handle this is the use of PV curtailment during overproduction and load shedding during periods of underproduction. The BESS being a high flexibility product, absorbs power during high ramp-down of the duck-curve and it discharges power during the high ramp-up of the duck-curve. This paper proposes an MPC-based optimal scheduling of generating units, BESS, load shedding and PV curtailment. Current researches on duck-curve handling generally model the economic dispatch in an open-loop system one day ahead [13], [14]. The models are formulated based on the forecast of the weather conditions, the predictions of the demand and electricity price, and the optimal unit dispatch is carried out in one cycle for each hour of the day ahead. The unit schedule based on these static methods may not be optimal in real time situations due sudden fluctuations of some factors in real time. In the MPC model, the operational schedule of the power-grid is formulated based on the predictions of future control actions for the EMS. These predictions are continuously updated in relation to the latest system state. The MPC-based model is compared with a non-MPC mixed integer linear programming (MILP). The optimization problem is formulated as an MILP problem based on MPC. Flexibility analysis is carried out on the model to show its effectiveness. The proposed model is simulated on the IEEE 24-bus reliability test system. The optimization is solved in GAMS optimizer using CPLEX solver. The main contributions of the paper can be summed up as follows:

1) The model uses MPC for producing control actions for charging and discharging of the BESS, load shedding, PV curtailment and unit scheduling. For the MPC model in this paper, 1-hour sampling time and 6 hours of planning horizon for the MPC are used. The model is tested for 24 hours because it coincides with the daily electricity demand and price.
2) A comparison is made with a non-MPC based MILP. This comparison is made to show the effectiveness of the proposed model.
3) A detailed flexibility analysis is carried out to show the effectiveness of the proposed EMS. The flexibility analysis showed that the EMS effectively handled the fast ramps of the duck curve.

The rest of the paper is organized as follows. Section II shows the formulation of the proposed model. Section III discusses the model predictive control. Section IV shows the formulation of the flexibility analysis. Section V describes the case study. Section VI discusses the results of the simulation. Section VII concludes the paper.

II. SYSTEM MODEL

The MPC-based EMS handles the fast ramps of the duck curve. The EMS dispatches the thermal units for balancing

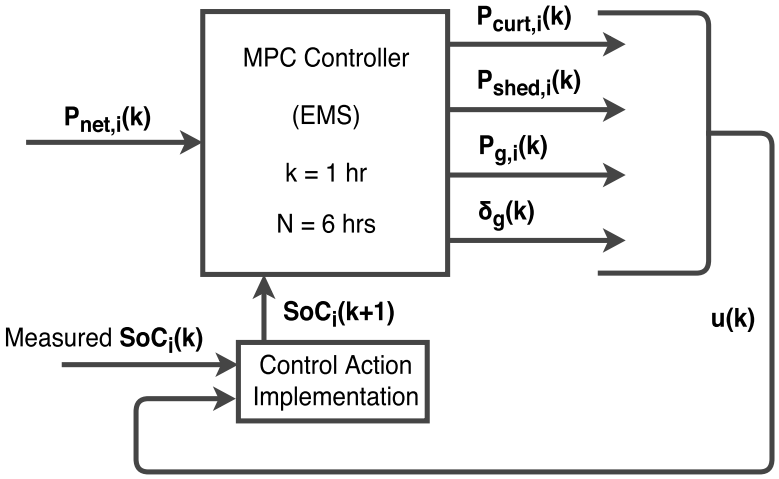

FIGURE 3. MPC Scheme.

the net load and schedules the BESS for minimizing PV curtailment and load shedding. The time horizon of the MPC is chosen to be $N = 6$, and the time-step k is 1 hour. The total time horizon for the operation of the power grid is 24 hours. Using 1-hr time-step and 6-hr time horizon for the MPC would give more accurate control actions prediction. The 1-hr time-step for the MPC is chosen as it matches the 1-hr time instant of unit commitment. Using 6-hr planning horizon would be faster than higher time steps like 24-hr. The main objective is to minimize the total operational cost (TOC). For each time step k, MPC optimizes the TOC for the time horizon N, while implementing only the first control action and updating the state of the system. This is done for every time instant t of the time horizon of the power system operation T. This is shown in Figure 3. The state-space MPC is a good candidate for powergrids. The state-space formulation can easily incorporate multivariable systems, which is the case for powergrids. With regards to the proposed model, the state vector $x(k)$ is the state of charge $SoC(k)$ of the BESS. The output $y(k)$ for power grids coincides with the state $x(k)$. The control vector $u(k)$ is the BESS power $P_{BESS,i}(k)$ which consists of the power flows that can be manipulated, namely, curtailed PV power $P_{curt,i}(k)$, load shed $P_{shed,i}(k)$, power supplied by the generators $P_g(k)$ and online status of the generating units $\delta_g(k)$. The disturbances $d(k)$ of the MPC are quantities that can be measured but not manipulated or controlled. The disturbances with regards to the proposed EMS are the solar PV output $P_{PV,i}(k)$ and load $P_{load,i}(k)$ which are represented by the net load $P_{net,i}(k)$. The BESS is only considered as the state variable because the MPC is developed to give an optimal UC of the power sources by making efficient management of the BESS. Since the optimization problem involves unit commitment, 1-hr timescale is used. This timescale synchronizes with the capacity of the BESS which is in MWh. Which means the BESS charges/discharges for 1 hour long before the next decision is made. The MPC dynamics can be defined in the state space equation shown in (1) below.

$$\begin{aligned} x(k+1) &= x(k) + u(k) + d(k) \\ y(k) &= x(k) \end{aligned} \tag{1}$$

With

$$\begin{aligned} x(k) &= SoC_i(k) \\ u(k) &= [P_{curt,i}(k)\ P_{shed,i}(k)\ P_g(k)\ \delta_g(k)]^T \\ d(k) &= P_{load,i}(k) - P_{PV,i}(k) = P_{net,i}(k) \\ y(k) &= x(k) \end{aligned}$$

The MPC-based model is formulated as follows. From equation of the state in (1), the BESS state is defined by (2).

$$\begin{aligned} SoC_i(k+1) &= SoC_i(k) + \eta P_{BESS,i}(k) \\ \eta &= \begin{cases} \eta_{ch}, & \text{if } P_{BESS,i}(k) > 0 \ (charging) \\ 1/\eta_{dis}, & \text{otherwise } (discharging) \end{cases} \end{aligned} \tag{2}$$

$P_{BESSi}(k)$ is defined by the power balance equation in (3).

$$\begin{aligned} P_{BESS,i}(k) = P_g(k) + P_{shed,i}(k) + P_{PV,i}(k) \\ - P_{curt,i}(k) - P_{load,i}(k) \end{aligned} \tag{3}$$

The rest of the system constraints are expressed as follows.

$$-E_i \le P_{BESS,i}(k) \le E_i \tag{4}$$

$$0 \le SoC_i(k) \le E_i \tag{5}$$

$$Fc_g(k) = a_g(P_g(k))^2 + b_g P_g(k) + c_g \quad \forall g \in N_g \tag{6}$$

$$P_g(k) - P_g(k-1) \le R_g^{up} \tag{7}$$

$$P_g(k-1) - P_g(k) \le R_g^{dn} \tag{8}$$

$$\delta_g(k) - \delta_g(k-1) \le \delta_g(\tau) \tag{9}$$

$$\delta_g(k-1) - \delta_g(k) \le 1 - \delta_g(\tau) \tag{10}$$

where $\tau = k+1,\ldots, \min(k + Ut_g - 1, T)$ for minimum up time. For minimum down time $\tau = \min(k + Dt_g - 1, T)$.

$$y_g(k) - z_g(k) = \delta_g(k) - \delta_g(k-1) \tag{11}$$

$$y_g(k) + z_g(k) \leq 1 \quad (12)$$
$$\delta_g(k), y_g(k), z_g(k), \in [0, 1] \quad (13)$$
$$Su_g(k) = C_g^{up} y_g(k) \quad (14)$$
$$Sd_g(k) = C_g^{dn} z_g(k) \quad (15)$$
$$P_g^{min} \leq P_g(k) \leq P_g^{max} \quad (16)$$
$$P_{curt,i}(k) = P_{PV,i}(k) T_{PV,i} - p_{pv,i}(k) \quad (17)$$
$$0 \leq p_{pv,i}(k) \leq P_{PV,i}(k) T_{PV,i}(k) \quad (18)$$
$$0 \leq P_{shed,i}(k) \leq P_{load,i}(k) \quad (19)$$
$$P_{ij}(k) = \frac{\theta_i(k) - \theta_j(k)}{X_{ij}} \quad ij \in l \quad (20)$$
$$-P_{ij}^{Rated} \leq P_{ij}(k) \leq P_{ij}^{Rated} \quad \forall i, j \in N_i \quad (21)$$

The cost function of the MPC-based EMS is defined by

$$TOC = min \sum_{t=1}^{T} \sum_{g=1}^{N_g} [Fc_g(t+k|t) + Su_g(t+k|t) + Sd_g(t+k|t) + C_{shed} P_{shed,i}(t+k|t) + C_{curt} P_{curt,i}(t+k|t)] \quad (22)$$

The BESS power limit is given by (4) [23]. The SOC limit is defined by (5). The fuel cost of the generating units is defined by (6) based on the formulations in [24], [27]. The ramp-up and ramp-down constraints of the units are defined by (7) and (8) respectively [25]. The minimum up and minimum down constraints are defined by (9) and (10) based on the formulation in [26]. The constraint in (9) defines the minimum up time in such a way that if a unit is turned on at time step k, that unit will remain on for the rest of either the time horizon or the unit's minimum up time, depending on which is shorter. For instance, if unit g is off at $(k-1)$, that is, $\delta_g(k-1) = 0$ and then turned on at k, that is, $\delta_g(k) = 1$, (9) will force all the binary optimization variables corresponding to the unit ON/OFF-state to be equal to 1 for next $Ut_g - 1$ or T. Constraints in (11) and (12) ensure that generator g is only in one state, that is, on or off at any given time step k. $\delta_g(k)$, $y_g(k)$ and $z_g(k)$ are defined as binary variables by (13). The start-up and shut-down costs of the units are defined by (14 and (15). The maximum and minimum generation limits of the units is defined in (16).

Sudden drop in demand causes challenges with units that are not flexible. Instead of shutting down these units or leaving them online and generating power in excess of the demand, the PV output is curtailed. The PV curtailment is modelled by (17) [27]. It defines the amount of PV output curtailed at time step k. The first term in the right hand side of (17) is the maximum possible solar energy that can be generated at time step k. The second term is the actual solar energy produced at time step k. During periods of over-production, the actual solar energy generated is controlled so that it is less than the maximum that can be generated. The difference between these two terms is the PV energy curtailed. The PV output at the buses is limited by (18).

The interruptible load constraint is defined by (19). It constitutes a certain quantity of load that can be interrupted at a cost. The equation shows the maximum amount of load that can be interrupted.

The optimal power flow (OPF) formulation is modelled by (20) and (21). The power injection into bus i is given by (20). The flow limit from bus i to bus j on the transmission line is given by (21), it limits the flow of the power between the buses.

The cost function of the MPC is defined by (22) which is the objective function of the optimization problem. The first term is the fuel cost of the units which is defined in (6). The second and third terms are the start-up and shut-down costs of the units, respectively. They are defined in (14) and (15) respectively. The second to the last term is the cost for load shedding. The last term of (22) is the PV curtailment cost. It is cost incurred as a result of curtailing the PV output.

A. NON-MPC BASED MILP OPTIMIZATION

The MILP consists of a linear objective function with a binary variable (generator status) and linear constraints. The MILP is of the form shown below.

$$min\ c^T x\ Ax = b\ (linear\ constraints)$$
$$l \leq x \leq u\ (bound\ constraints)$$

All the x take integer values.

In the non-MPC MILP formulation, the objective function and constraints are similar to that of the MPC based optimization without the time steps. The optimization is performed for the 24-hr planning horizon in one cycle not in steps. Time instant of 1-hr is used in the simulation. A comparison is made between the non-MPC MILP optimization and the MPC-based optimization is done in Section VI.

The MPC-based model in this paper is formulated using MILP. The timescale of the MPC based formulation is slow enough to be compared with the non-MPC based formulation. Also, since the timescales of both the non-MPC MILP optimization and that of the MPC coincide, the MILP optimization is embedded into the MPC giving rise to MILP-based MPC optimization. Using the MILP formulation, the feedback control action of the MPC can be applied which produces future control actions. For each time instant of the MPC, an MILP optimization is solved.

III. MODEL PREDICTIVE CONTROL

The MPC scheme consists of computing existing system knowledge and future predictions online in order to obtain the control actions to a system instead of using offline static parameters [28]. The MPC consists of time steps which constitute a finite time horizon. For every time step, the system is optimized for a finite time horizon by producing a sequence of control action, and implementing only the first control action [21]. Then the system enters the next time step with an updated system state and future knowledge, and the above calculation is repeated. MPC is a closed loop control action as it continuously modulates control actions to correct

inaccurate predictions. The methodology of the MPC control strategy is carried out in the following steps [22].

1) The future outputs for a finite time horizon N, are forecasted by the MPC at time instant t. The predicted output $y(t+k|t)$, for $k = 1 \ldots N$, depends on the past input and output up to time instant t, and on the future control signal $u(t+k|t)$, $k = 0 \ldots N-1$.
2) The control signal is computed based on optimization of the objective. The control signal keeps the output as close as possible to the reference trajectory (objective).
3) The current control signal $u(t|t)$ is implemented while the next control signals are discarded, this is because at the next time step $k = 1$, the output $y(t+1)$ is known. Step 1 is repeated with this new values of the output $y(t+1|t)$ and state $x(t+1|t)$. Therefore, the control signal $u(t+1|t+1)$ is calculated.

IV. FLEXIBILITY ANALYSIS

Flexibility is the probability that the available flexible resources would satisfy the demand as at when needed without curtailment and load loss. Lack of upward flexibility results in load loss, while the lack of downward flexibility causes RES curtailment. The flexibility index used in this paper is the period of flexibility deficit (PFD) [29]. This shows periods where the system ramping is greater than the ramping provided by the system's flexibility sources. This is expressed as follows [30]:

$$P_{def}(t) = R_{net}(t) - (Flex_{on}(t) + Flex_{off}(t)) \tag{23}$$

where, the net load ramp is defined by equation (24) below:

$$R_{net}(t+1) = P_{net}(t+1) - P_{net}(t) \tag{24}$$

The online and offline available flexibility are given by equations (25) and (26).

$$Flex_{on}(t) = \sum_{g} x_g(t) min(R_g^{up}, P_g^{max} - P_g(t)) \tag{25}$$

$$Flex_{off}(t) = \sum_{g} (1 - x_g(t)) min(R_g^{up} * (1 - y_g), P_g^{min}) \tag{26}$$

For negative values of the net load ramp, $P_{def(t)}$ becomes:

$$P_{def}(t) = |P_{net}(t)| - Flex_{on}(t) \tag{27}$$

$$Flex_{on}(t) = \sum_{g} x_g(t) min(R_g^{dn}, P_g(t) - P_g^{min}) \tag{28}$$

Online flexibility is the ramping capability of the online power sources in handling the ramps of the net load at time instant t. Offline flexibility consists of available offline units that can be started in order to meet up with a ramp up in demand at time instant t.

V. CASE STUDY

The proposed formulation is simulated on the IEEE 24-bus RTS. The model is simulated in GAMS software using CPLEX solver. Historical solar data of Dammam, Saudi Arabia, is used for the summer season of 2017, 2018 and 2019. The average of a daily solar output is taken as the PV output data. Table 1 shows the parameters of the thermal units for the IEEE 24-bus. The transmission lines data and load data are provided in [31]. A 6-hr MPC time horizon with 1-hr time step is used. The case study is conducted for 24 hours. This is chosen as it coincides wih the daily customer demand and daily cycle of the solar energy. The random variables of the load and PV are not considered because historical values are used. The MPC controller uses this data to predict the control actions for successive time steps. In order to illustrate a high level of PV penetration, six 200 MW solar PVs are integrated at buses 8, 10, 13, 15, 18 and 20 which resulted in a duck curve pattern as shown in Figure 4. BESSs of 20 MWh capacities are initially integrated to each bus containing the solar PV. The capacity of the PVs is later changed to 230 MW at each bus after carrying out sensitivity analysis in Section VI-C as shown in Figure 5 and the BESS capacities at each bus is changed to 130 MWh.

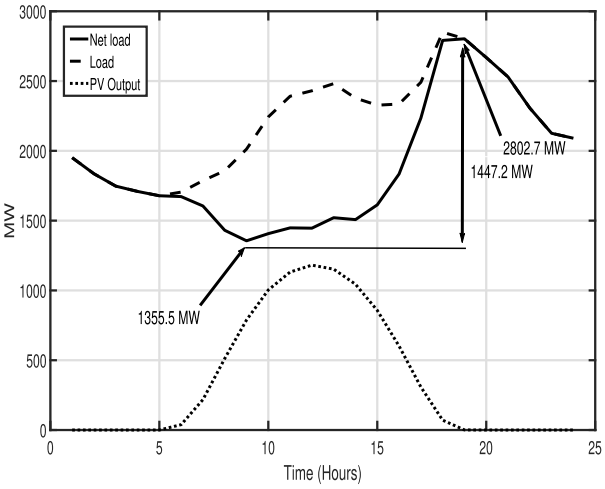

FIGURE 4. Duck curve.

The cost of the load shedding at every bus for each hour is fixed to 500 $/kWh [32]. The PV curtailment cost is calculated as in [3]. The PV curtailment cost is 286 $/kWh. The BESS characteristics are shown in Table 2. The total capacity of the thermal units is 3,375 MW and peak of the net load is 2,802.7 MW. Although the total capacity of the thermal units is greater than the peak of the net load, BESSs, load shedding and PV curtailment are used in the model because the thermal units can not respond to the fast ramps of the duck curve. In order to show the effectiveness of the model, the results from the MPC based EMS is compared to that of an MILP optimization with no MPC.

VI. RESULTS

A. MILP OPTIMIZATION

This is the open loop solution to the mixed integer optimization. In this simulation, the MPC is not implemented. It based on the solution to the MILP optimization of the unit commitment problem. After the simulation is run, the optimal unit commitment is shown in Figure 6. The SOC level is

TABLE 1. Parameters of the Thermal Units.

Unit	Node	Pmin (MW)	Pmax (MW)	Ramp down (MW/h)	Ramp up (MW/h)	Ut (h)	Dt (h)
1	18	100	400	47	47	1	1
2	21	100	400	47	47	1	1
3	1	30.4	152	14	14	8	4
4	2	30.4	152	14	14	8	4
5	15	54.25	155	21	21	8	8
6	16	54.25	155	21	21	8	8
7	23	108.5	310	21	21	8	8
8	23	140	350	28	28	8	8
9	7	75	350	49	49	8	8
10	13	206.85	591	21	21	12	10
11	15	12	60	7	7	4	2
12	22	0	300	35	35	0	0

TABLE 2. Typical BESS characteristics.

Configuration	Total capital cost per power ($/kW)	Total capital cost per energy ($/kWh)	Round trip efficiency (%)
Li-ion	874	973	95

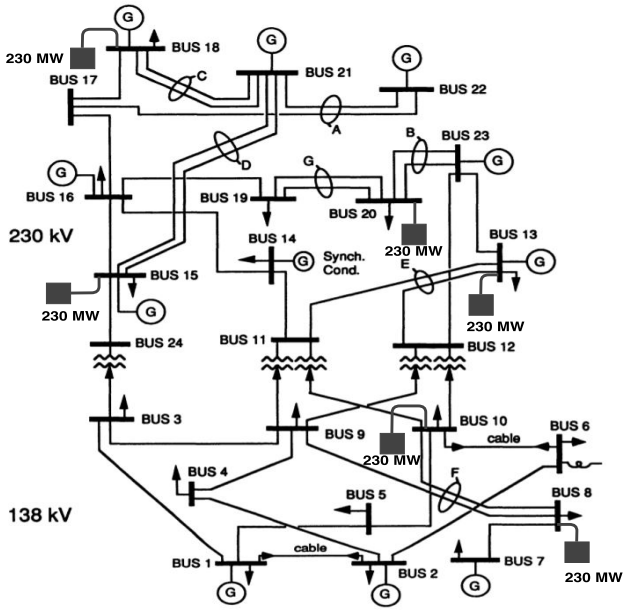

FIGURE 5. Allocation of solar PVs on the IEEE 24-bus RTS.

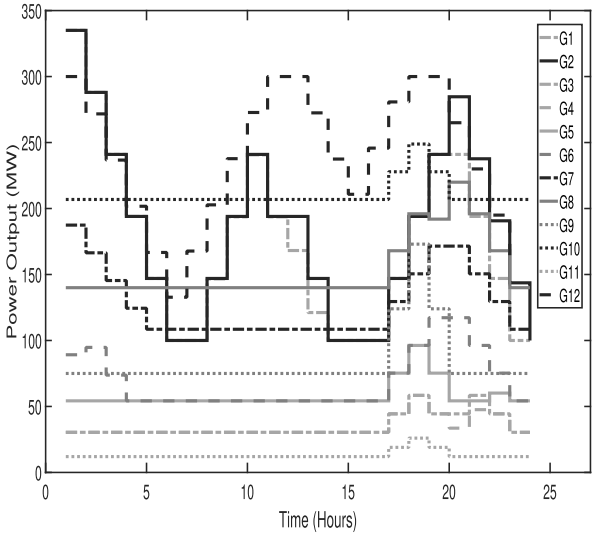

FIGURE 6. Unit commitment for non-MPC MILP.

shown in Figure 7. The total operational cost for 24 hours is $ 340,235.

B. MPC-BASED

This is the closed loop solution to the optimization problem based on MPC. The model proposed in (2) to (22) is implemented for 24-hr planning horizon. The time horizon for each hour of the 24-hr MPC based optimization is 6 hours. In each hour of the optimization, control actions are optimized for the next 6 hours while implementing only the first control actions. After the simulation, the optimal unit commitment is shown in Figure 8. The SOC of the BESSs is shown in Figure 9. The total operational cost is less than that of the MILP optimization.

In all the simulations, the system is operated with the same load profiles, generating units, PV capacity and BESS capacity. The main purpose of the optimization is to tackle the duck curve fast ramps by maintaining the energy balance between production and consumption.

The SOC level of the MPC-based optimization is more evenly distributed along the planning horizon compared to that of the MILP optimization. In the MPC-based SOC is higher in the early morning and lower later in the day. This is because of steeper slopes of the duck curve and higher demand later in the day. After performing sensitivity analysis and determining the right size of the BESS (130 MWh), the TOC of the MPC-based optimization is $ 284,752. Using the same size of BESS (130 MWh) for the non-MPC MILP optimization, the TOC is $ 340,235. The MPC based EMS is proven to be effective as it handles the fast ramps of the duck curve at a cost that is less than the non-MPC based MILP optimization.

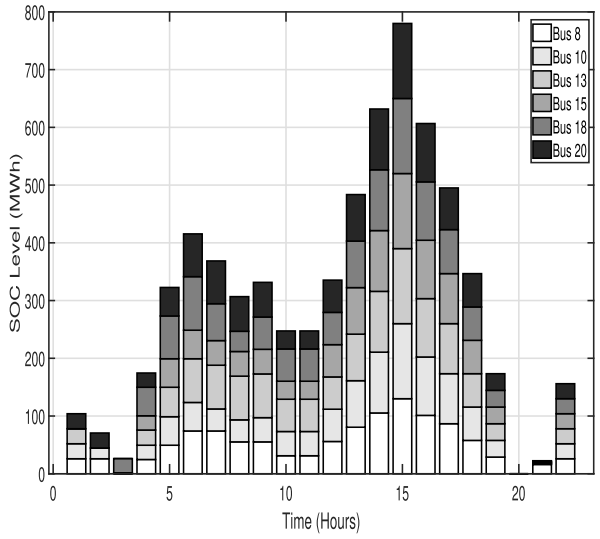

FIGURE 7. SOC for non-MPC MILP.

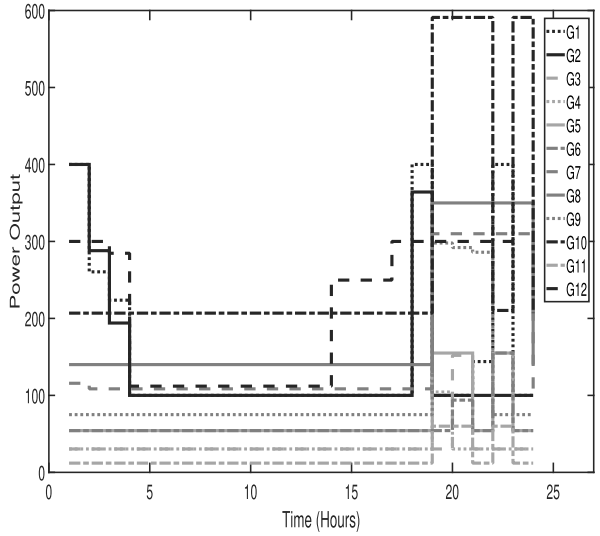

FIGURE 8. Unit commitment for MPC-based EMS.

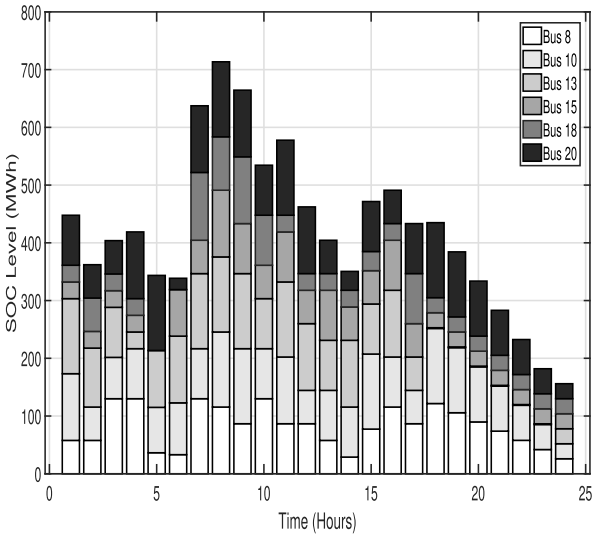

FIGURE 9. SOC for MPC-based EMS.

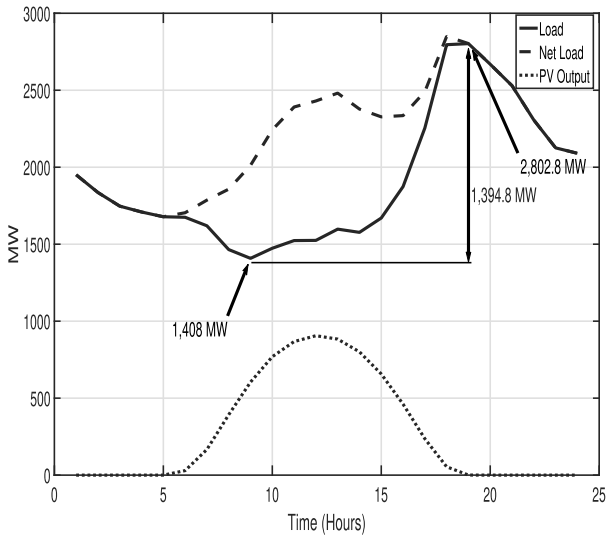

FIGURE 10. Duck curve with 48.42 % penetration.

C. SENSITIVITY ANALYSIS

Sensitivity analysis is carried out to find the effects of varying the PV capacity and size of the BESS on the TOC. An initial optimization is carried out using PVs of 200 MW each at buses 8, 10, 13, 15, 18 and 20 and BESSs of 20 MWh each at buses 8, 10, 13, 15, 18 and 20. The size of the PV at the buses is varied from 10 MW to 280 MW. The results are shown in Table 3. Increase in the PV capacity decreases the TOC. A point is reached where further increase in PV penetration (230MW capacity, 48.42 % penetration) increases the TOC as shown Table 3. This is as result of the net load having steeper slopes (faster ramps). Thus, 230 MW PVs are allocated each at buses 8, 10, 13, 15, 18 and 20. The resulting duck curve (net load) is shown in Figure 10.

Using PVs of 230 MW each at buses 10, 13, 15, 18 and 20, the BESS size is varied. The effect of the variation of the BESS is shown in Figure 12. Increase in the size of the BESS decreases the TOC. With 130 MWh BESSs each at buses 10, 13, 15, 18 and 20, the minimum TOC ($ 284,752) is reached where increase the size of the BESS results in no further decrease in the TOC as shown in Figure 12. As a result, 130 MWh BESSs are used and the SOC level is shown in Figure 12. The MPC-based optimization is carried out using 130 MWh BESSs and 230 MW PVs.

D. FLEXIBILITY ANALYSIS

Flexibility assessment is carried out on the model to show the effectiveness of the flexibility of the generating units and BESSs in tackling the fast ramps of the duck curve. The flexibility analysis is carried out based on (23) to (28).

1) NO BESS

The flexibility analysis is carried out with 230 MW PVs without BESS. Due the to fast ramps of the duck curve and

TABLE 3. Sensitivity of PV capacity relative to TOC for 24 hours.

PV unit (MW)	Total PV capacity (MW)	Penetration (%)	TOC ($)
10	60	2.11	450,709
20	120	4.21	440,837
30	180	6.32	431,187
40	240	8.42	421,974
50	300	10.53	412,985
60	360	12.63	403,245
70	420	14.74	393,814
80	480	16.84	384,383
90	540	18.95	380,394
100	600	21.05	373,128
110	660	23.16	365,862
120	720	25.26	358,596
130	780	27.37	351,329
140	840	29.47	344,063
150	900	31.58	336,797
160	960	33.68	336,744
170	1,020	35.79	330,346
180	1,080	37.89	321,271
190	1,140	40	312,197
200	1,200	42.11	318,522
210	1,260	44.21	314,936
220	1,320	46.32	311,825
230	1,380	48.42	308,715
240	1,440	50.53	318,553
250	1,500	52.63	369,118
260	1,560	54.74	436,257
270	1,620	56.84	509,311
280	1,680	58.95	592,794

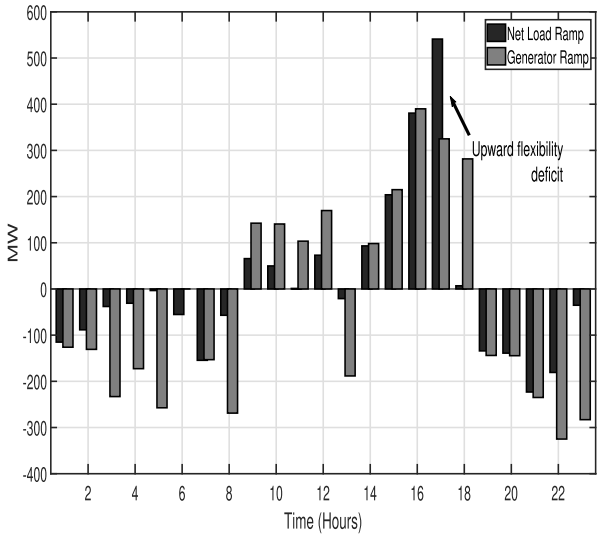

FIGURE 11. System flexibility with no BESS.

limited flexibility of the generating units, flexibility deficit is recorded as shown in Figure 11. Upward flexibility deficit is recorded as a result of 216.1 MW load shedding. The load shedding is as a result of the generating units limited flexibility to quickly ramp up in response to the duck curve fast ramp.

2) FLEXIBILITY OF THE MPC-BASED MODEL

The MPC-based model optimally scheduled the generating units and the BESS. No PFD is recorded for the 24 hour planning horizon. This is as result of the fast ramps of the net load being equally met by the flexibility of the generating

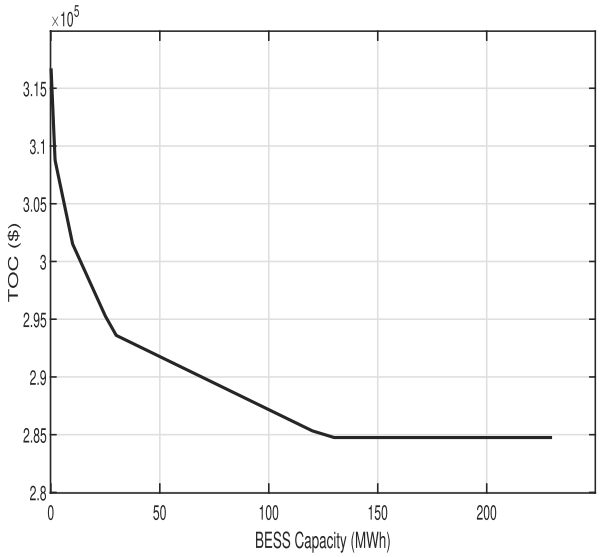

FIGURE 12. Sensitivity of BESS capacity for 24 hours.

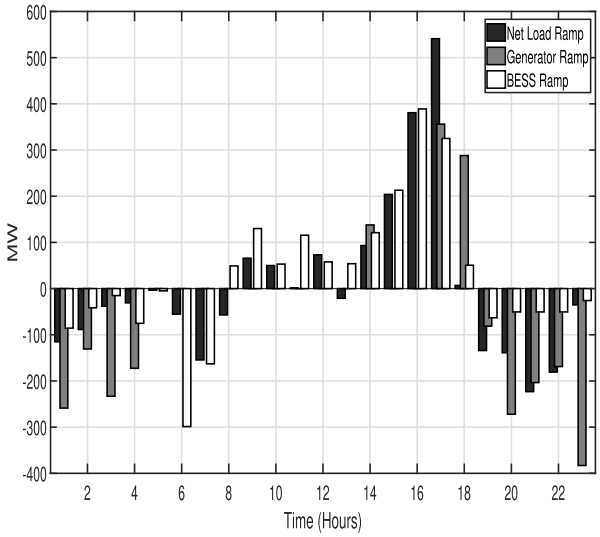

FIGURE 13. Flexibility of the generating units and BESS.

units and BESSs. Figure 13 shows the net load ramps, and the available flexibility of generating units and BESS for each hour t of the planning horizon. As shown in the figure, the available flexibility of the generating units and BESS is greater than the net load ramps for each hour t. The flexibility analysis carried out on the model shows the that the proposed model is effective because there is no period of flexibility deficit through out the planning period.

The BESS is sufficient enough to provide the necessary charging/discharging actions as shown in the sensitivity and flexibility analyses. The flexibility analysis also shows that for all the time instants, the ramps of the net load are being handled by the system's flexibility. In case the BESS charging and discharging actions are not sufficient, the EMS would use PV curtailment and load shedding to meet the ramping requirements. The control actions of the MPC modified the duck curve. The high ramps of the duck are reduced. This

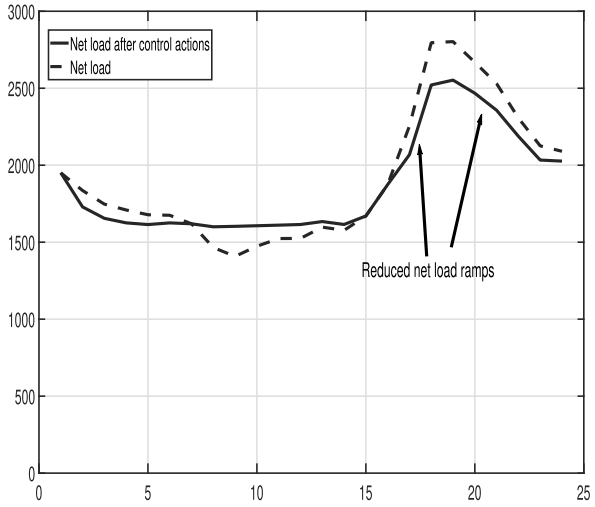

FIGURE 14. **Modified duck curve.**

eliminated load shedding. The modified duck curve is shown in Figure 14.

VII. CONCLUSION

In a power system with high PV penetration, a model was developed based on MPC to handle the duck curve phenomenon. The fast ramps of the duck curve are effectively handled by the EMS. The MPC-based EMS handled the fast ramps using BESS, load shedding and PV curtailment. A case study is carried out on a 24-bus RTS system to simulate the model. The flexibility analysis carried out shows that the proposed model is effective in handling the fast ramps of the duck curve while minimizing the total operation cost. This is evident as there is no period of flexibility deficit in the entire planning horizon. In comparison with non-MPC based MILP, the MP-based optimization is more economical in handling the duck curve fast ramps.

REFERENCES

[1] H. A. Aalami and S. Nojavan, "Energy storage system and demand response program effects on stochastic energy procurement of large consumers considering renewable generation," *IET Gener., Transmiss. Distrib.*, vol. 10, no. 1, pp. 107–114, Jan. 2016.

[2] E. Dall'Anese, S. V. Dhople, and G. B. Giannakis, "Photovoltaic inverter controllers seeking AC optimal power flow solutions," *IEEE Trans. Power Syst.*, vol. 31, no. 4, pp. 2809–2823, Jul. 2016.

[3] H. Kikusato, Y. Fujimoto, S.-I. Hanada, D. Isogawa, S. Yoshizawa, H. Ohashi, and Y. Hayashi, "Electric vehicle charging management using auction mechanism for reducing PV curtailment in distribution systems," *IEEE Trans. Sustain. Energy*, vol. 11, no. 3, pp. 1394–1403, Jul. 2020.

[4] M. Obi and R. Bass, "Trends and challenges of grid-connected photovoltaic systems – a review," *Renew. Sustain. Energy Rev.*, vol. 58, pp. 1082–1094, May 2016.

[5] P. Denholm, M. O'Connell, G. Brinkman, and J. Jorgenson, "Overgeneration from solar energy in california. a field guide to the duck chart," Nat. Renew. Energy Lab. (NREL), Golden, CO, USA, Tech. Rep. NREL/TP-6A20-65023, Nov. 2015.

[6] N. Kumar, S. Venkataraman, D. Lew, G. Brinkman, D. Palchak, and J. Cochran, "Retrofitting fossil power plants for increased flexibility," in *Proc. Amer. Soc. Mech. Eng., Power Division (Publication) POWER*, 2014, pp. 1–9.

[7] Q. Hou, N. Zhang, E. Du, M. Miao, F. Peng, and C. Kang, "Probabilistic duck curve in high PV penetration power system: Concept, modeling, and empirical analysis in China," *Appl. Energy*, vol. 242, pp. 205–215, May 2019, doi: 10.1016/j.apenergy.2019.03.067.

[8] X. Zhu, J. Yang, Y. Liu, C. Liu, B. Miao, and L. Chen, "Optimal scheduling method for a regional integrated energy system considering joint virtual energy storage," *IEEE Access*, vol. 7, pp. 138260–138272, 2019.

[9] N. Zhang, X. Lu, M. B. McElroy, C. P. Nielsen, X. Chen, Y. Deng, and C. Kang, "Reducing curtailment of wind electricity in China by employing electric boilers for heat and pumped hydro for energy storage," *Appl. Energy*, vol. 184, pp. 987–994, Dec. 2016.

[10] J. Zhang and Q. Zhang, "Feasibility and simulation study of high-rise building micro-grid with PV and mini-hydro pumping," in *Proc. IEEE Power Energy Soc. Gen. Meeting*, Vancouver, BC, Canada, Jul. 2013, pp. 1–5.

[11] P. Chaudhary and M. Rizwan, "Energy management supporting high penetration of solar photovoltaic generation for smart grid using solar forecasts and pumped hydro storage system," *Renew. Energy*, vol. 118, pp. 928–946, Apr. 2018.

[12] C. Le Floch, F. Belletti, and S. Moura, "Optimal charging of electric vehicles for load shaping: A dual-splitting framework with explicit convergence bounds," *IEEE Trans. Transport. Electrific.*, vol. 2, no. 2, pp. 190–199, Jun. 2016.

[13] H. O. R. Howlader, M. Furukakoi, H. Matayoshi, and T. Senjyu, "Duck curve problem solving strategies with thermal unit commitment by introducing pumped storage hydroelectricity & renewable energy," in *Proc. IEEE 12th Int. Conf. Power Electron. Drive Syst. (PEDS)*, Dec. 2017, pp. 502–506.

[14] H. O. R. Howlader, M. M. Sediqi, A. M. Ibrahimi, and T. Senjyu, "Optimal thermal unit commitment for solving duck curve problem by introducing CSP, PSH and demand response," *IEEE Access*, vol. 6, pp. 4834–4844, 2018.

[15] F. R. Segundo Sevilla, D. Parra, N. Wyrsch, M. K. Patel, F. Kienzle, and P. Korba, "Techno-economic analysis of battery storage and curtailment in a distribution grid with high PV penetration," *J. Energy Storage*, vol. 17, pp. 73–83, Jun. 2018.

[16] M. Afzal, Q. Huang, W. Amin, K. Umer, A. Raza, and M. Naeem, "Blockchain enabled distributed demand side management in community energy system with smart homes," *IEEE Access*, vol. 8, pp. 37428–37439, 2020.

[17] B. M. Sanandaji, T. L. Vincent, and K. Poolla, "Ramping rate flexibility of residential HVAC loads," *IEEE Trans. Sustain. Energy*, vol. 7, no. 2, pp. 865–874, Apr. 2016.

[18] J. Lazar, *Teaching the 'Duck' to Fly*, 2nd ed. Montpelier, VT, USA: The Regulatory Assistance Project, 2016. [Online] Available: http://www.raponline.org/document/download/id/7956

[19] A. A. Z. Diab, H. M. Sultan, I. S. Mohamed, O. N. Kuznetsov, and T. D. Do, "Application of different optimization algorithms for optimal sizing of PV/wind/diesel/battery storage stand-alone hybrid microgrid," *IEEE Access*, vol. 7, pp. 119223–119245, 2019.

[20] J. Wu, X. Ai, J. Hu, and Z. Wu, "Peer-to-peer modeling and optimal operation for prosumer energy management in intelligent community," *Dianwang Jishu/Power Syst. Technol.*, 2020, doi: 10.13335/j.1000-3673.pst.2019.0646.

[21] H. Iranmanesh and A. Afshar, "MPC-based control of a large-scale power system subject to consecutive pulse load variations," *IEEE Access*, vol. 5, pp. 26318–26327, 2017.

[22] C. Bordons, F. Garcia-Torres, and M. A. Ridao, *Model Predictive Control of Microgrids*. Cham, Switzerland: Springer, 2020, pp. 25–43.

[23] T. M. Masaud and E. F. El-Saadany, "Correlating optimal size, cycle life estimation, and technology selection of batteries: A two-stage approach for microgrid applications," *IEEE Trans. Sustain. Energy*, vol. 11, no. 3, pp. 1257–1267, Jul. 2020.

[24] M. Sufyan, N. Abd Rahim, C. Tan, M. A. Muhammad, and S. R. Sheikh Raihan, "Optimal sizing and energy scheduling of isolated microgrid considering the battery lifetime degradation," *PLoS ONE*, vol. 14, no. 2, Feb. 2019, Art. no. e0211642.

[25] D. Pozo, J. Contreras, and E. E. Sauma, "Unit commitment with ideal and generic energy storage units," *IEEE Trans. Power Syst.*, vol. 29, no. 6, pp. 2974–2984, Nov. 2014.

[26] A. Ahmadi, A. E. Nezhad, and B. Hredzak, "Security-constrained unit commitment in presence of lithium-ion battery storage units using information-gap decision theory," *IEEE Trans. Ind. Informat.*, vol. 15, no. 1, pp. 148–157, Jan. 2019.

[27] A. Soroudi, *Power System Optimization Modeling in GAMS*. Cham, Switzerland: Springer, 2017.

[28] E. Mayhorn, K. Kalsi, M. Elizondo, W. Zhang, S. Lu, N. Samaan, and K. Butler-Purry, "Optimal control of distributed energy resources using model predictive control," in *Proc. IEEE Power Energy Soc. Gen. Meeting*, Jul. 2012, pp. 1–8.
[29] E. Lannoye, D. Flynn, and M. O'Malley, "Transmission, variable generation, and power system flexibility," *IEEE Trans. Power Syst.*, vol. 30, no. 1, pp. 57–66, Jan. 2015.
[30] E. Lannoye, D. Flynn, and M. O'Malley, "Assessment of power system flexibility: A high-level approach," in *Proc. IEEE Power Energy Soc. Gen. Meeting*, Jul. 2012, pp. 1–8.
[31] C. Grigg, P. Wong, P. Albrecht, R. Allan, M. Bhavaraju, R. Billinton, Q. Chen, C. Fong, S. Haddad, S. Kuruganty, W. Li, R. Mukerji, D. Patton, N. Rau, D. Reppen, A. Schneider, M. Shahidehpour, and C. Singh, "The IEEE reliability test system-1996. A report prepared by the reliability test system task force of the application of probability methods subcommittee," *IEEE Trans. Power Syst.*, vol. 14, no. 3, pp. 1010–1020, Aug. 1999, doi: 10.1109/59.780914.
[32] R. Hemmati and H. Saboori, "Short-term bulk energy storage system scheduling for load leveling in unit commitment: Modeling, optimization, and sensitivity analysis," *J. Adv. Res.*, vol. 7, no. 3, pp. 360–372, May 2016.

SULAIMAN S. AHMAD (Student Member, IEEE) was born in Kano, in October 1990. He received the B.Sc. degree in electrical engineering from Bayero University Kano, Kano, Nigeria, in 2015. He is currently pursuing the M.Sc. degree with the Electrical Engineering Department, King Fahd University of Petroleum and Minerals (KFUPM), Dhahran, Saudi Arabia. He is also a Graduate Student Researcher with the King Abdullah City for Atomic and Renewable Energy (K. A. CARE) Energy Research and Innovation Center, Dhahran. His research interests include power system planning and optimization, renewable energy integration, and energy storage systems planning. He received the Best Student Poster Award in grid integration section from the K. A. CARE Annual Review in November 2019.

FAHAD SALEH AL-ISMAIL (Senior Member, IEEE) received the B.Sc. and M.Sc. degrees in electrical engineering from the King Fahd University of Petroleum and Minerals (KFUPM), Dhahran, Saudi Arabia, in 2009 and 2012, respectively, and the Ph.D. degree in electrical engineering from Texas A&M University at College Station, TX, USA, in December 2016. He is the Director of the Center for Environment and Water (CEW), Research Institute (RI), and an Assistant Professor at the Department of Electrical Engineering, KFUPM. Before he was appointed as the Director of CEW, he was the Director of Energy Research and Innovation Center, KFUPM, sponsored by the King Abdullah City for Atomic and Renewable Energy (K.A.CARE), from January 2019 to August 2020. He also offers various courses in energy efficiency, demand-side management, power system operation and control, and power system planning. His research interests include power system planning and reliability, renewable energy integration, energy storage system planning and operation, demand-side management modeling with intermittent resources, and uncertainty representation of renewable energy.

ABDULLAH A. ALMEHIZIA (Member, IEEE) received the B.Eng. degree in electrical engineering from King Saud University, Riyadh, Saudi Arabia, in 2010, the M.Eng. degree in electrical engineering from the University of Calgary, Calgary, AB, Canada, in 2014, and the Ph.D. degree in electrical engineering from Texas A&M University, College Station, TX, USA, in 2018. He is currently the Director of the National Center for Electrical Systems Technology, King Abdulaziz City for Science and Technology (KACST), where he also works in electrical distribution networks monitoring systems. His main research interests include renewable energy resources integration and optimization and power system planning, operation, and economics.

MUHAMMAD KHALID (Senior Member, IEEE) received the Ph.D. degree in electrical engineering from the School of Electrical Engineering and Telecommunications (EE and T), University of New South Wales (UNSW), Sydney, NSW, Australia, in 2011. He was a Postdoctoral Research Fellow for a period of three years and a Senior Research Associate with the School of EE and T, Australian Energy Research Institute, UNSW, for a period of two years. He is currently an Assistant Professor with the Electrical Engineering Department, King Fahd University of Petroleum and Minerals (KFUPM), Dhahran, Saudi Arabia. He is also a Researcher with the King Abdullah City for Atomic and Renewable Energy (K. A. CARE) Energy Research and Innovation Center, Dhahran. He has authored/coauthored several journal articles and conference papers in control and optimization for renewable power systems. His current research interests include optimization and control of battery energy storage systems for large-scale grid-connected renewable power plants (particularly wind and solar), distributed power generation and dispatch, hybrid energy storage, EVs, and smart grids. He was a recipient of the Highly-Competitive Postdoctoral Writing Fellowship from UNSW in 2010. He also received the Prestigious K. A. CARE Fellowship. He serves as a Reviewer for numerous international journals and conferences.